

CO₂ Purification using an Aqueous Amine Absorbent in the Syngas

^[1] Jeong Ho Choi, ^[2] Soung Hee Yun, ^[3] Sung Chan Nam, ^[4] Il Soo Chun, ^[5] Jin Young Jung, ^[6] Yeo Il Yoon, ^[7] Jung-Hyun Lee

^{[1][2][3][4][5][6]} Greenhouse Gas Laboratory, Climate Change Research Division, Korea Institute of Energy Research, 152 Gajeong-ro, Yuseong-gu, Daejeon 34129, Korea

^{[1][7]} Department of Chemical & Biological Engineering, Korea University, 145 Anam-dong, Seongbuk-gu, Seoul 02841, Korea

Abstract:-- The acetic acid production using syngas in the BP chemical process showed superior performance compared to using rhodium-based catalyst. However, CO₂ in the syngas causes poison of the promoted-iridium and the performance of the catalyst degrades. Therefore, CO₂ must remain at extremely low concentration below 20 ppmv. In this study, we try to develop the new CO₂ capturing absorbent for replacing with BASF a-MDEA (activated MDEA). The absorption performance of amine absorbents was evaluated to keep the CO₂ concentration low and the applicability of the absorbent for acetic acid production process was evaluated. A continuously stirred-tank reactor and differential reaction calorimeter were used to measure the CO₂ absorption capacity and heat of reaction, respectively.

As results among the amine absorbents, KIERSOL-N and KIERSOL-P showed better performance in both CO₂ absorption capacity and heat of reaction than MEA's results and a-MDEA's results.

Index Terms— Acetic acid, Gas purification, CO₂ control, amine absorbent.

I. INTRODUCTION

Acetic acid is used as a raw material for fine chemical products such as vinyl acetate and acetic acid ester. It is also a chemical substance widely used in such as terephthalic acid solution and dye [1]. A projected increase in the consumption of acetic acid has been reported at 4.0–4.5 % annually in China through 2020. China is expected to consume an average of 3–4 % of worldwide production [2]. The annual production of acetic acid is about 11.8 Mt/year, of which the production of acetic acid based on the methanol carbonylation technology is equivalent to about 80% [3],[4]. Processes for production of acetic acid using methanol carbonylation technology generally use noble metal catalysts such as iridium and ruthenium. The acetic acid production process based on ruthenium was widely used after being commercialized by Monsanto in 1970 [5]. In 1996, BP Chemical developed an improved methanol carbonylation process based on promoted iridium-iodide catalyst [6]. However, Bu₄NI catalyst has the disadvantage that the iodide poisons the catalyzed reaction and reduces the reaction rate to 67% or less [7]. Therefore, many researchers have tried to improve the performance of catalyst using the iridium-complex [8],[9]. The annual production of acetic acid using iridium-complex catalyst was very high, but the problem of catalyst poisoning by CO₂ occurred. Therefore, the use of CO₂ capture technology was required to separate CO₂ from the

syngas.

A primary syngas manufactured through partial oxidation is commonly used to produce acetic acid [10]. The primary syngas is composed of CO (60–70 %), H₂ (30–40 %), CO₂ (1–5 %), along with CH₄ and other impurities. The H₂S present in the syngas was removed via desulfurizer, and the CO/H₂ was separated by the pressure swing adsorption process (PSA). The CO₂ in the syngas was removed by CO₂ capture technology, and the remaining CO₂ should be limited to less than 20 ppm to prevent poisoning of the catalyst. Thus, high-level purification of CO₂ is very important for increasing efficiency in the acetic acid production process. The CO₂ capture technology used in the petrochemical industry was developed for gas purification purposes. In particular, the gas purification method using amines has been widely used commercially since its development by R. Richards in 1930 [11]. The typical amine absorbents are monoethanolamine (MEA), diethanolamine (DEA), and N-methyldiethanolamine (MDEA) [12]. Amines are classified as primary, secondary, or tertiary amines depending on their structural characteristics. MEA is a primary amine, which has the advantages of low cost and high CO₂ absorption rate, but the disadvantages of low CO₂ capacity, thermal degradation, oxidative degradation, corrosion, etc [13]–[16]. DEA has a relatively lower CO₂ absorption rate than MEA does. MDEA is an absorbent used in early 1950, and has the advantage of treating H₂S and CO₂ simultaneously

[17], but it has the disadvantage of a very low absorption rate [18]. In the 2000s, gas purification technology using amines was considered for application in carbon capture and storage (CCS) technology. The core technology of CCS is absorbents, and CO₂ capacity, absorption rate and regeneration energy for CO₂ capture process using a wet absorption method have been studied to evaluate the performance of absorbents. Recently, alternative absorbents in the form of cyclic amines such as piperazine (PZ) and 2-methylpiperazine (2MPZ) have been reported for use as commercial absorbents in power plants because of their advantages of low absorption heat, high CO₂ capacity and rapid reaction rate [19],[20]. In this study, various cyclic absorbents with potassium carbonate were evaluated to control CO₂ in an acetic acid production process, one of petrochemicals. The CO₂ absorption capacity and heat of reaction were measured and compared with MEA (30 wt%) and activated MDEA (α -MDEA; 40 wt% MDEA + 5 wt% PZ), in order to confirm the applicability of cyclic amines. When each absorbent was used, the concentration of emitted CO₂ was kept below 20 ppm.

II. EXPERIMENT

The CO₂ absorption capacity and heat of reaction were measured using a continuously stirred-tank reactor (CSTR) and differential reaction calorimeter (DRC), respectively. The mixed gases (3 vol% CO₂ / balanced N₂) used in the DRC experiment were purchased from Special Gas Co. in Korea. The CSTR experiments were conducted by mixing N₂ (99.9999%) and CO₂ (99.9999%) gas. MEA (2-aminoethanol; $\geq 99\%$), PZ (piperazine; 99.0%), and potassium carbonate (K₂CO₃; 99.5%) were from Samchun Chemicals. MDEA (N-methyldiethanolamine; ≥ 99.0) from Sigma Aldrich and 2MPZ (2-methylpiperazine; 98%) from Acros Organics were also used. The following four different absorbents mixed with deionized water were used for the experimental comparison of performance:

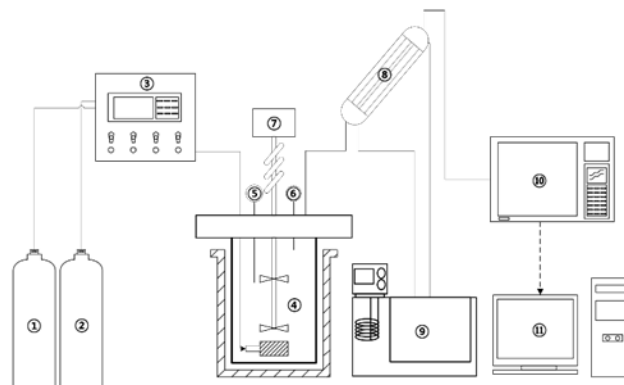
1) Commercially available and widely used aqueous 30 wt% MEA solution, 2) α -MDEA for simultaneous treatment of H₂S and CO₂, 3) KIERSOL-N (a brand of the Korea Institute of Energy Research) [21], and 4) KIERSOL-P (a brand used for petrochemical applications).

III. EXPERIMENTAL SETUP AND PROCEDURE

A. Continuously stirred-tank reactor (CSTR)

The experimental apparatus used in this study is shown in Fig. 1. The pressure in the CSTR was maintained at 9.50 to 9.52 bar to simulate the absorber of the CO₂ capture process. In the CO₂ absorption capacity experiment, the measurement was made by supplying 500 mL of absorbent to a reactor with an internal volume of 750 mL. The

reaction temperature



during the experiment was controlled by a water bath. CO₂ was supplied using a sparger to maximize contact with the surface of the absorbent; the stirring was done at a constant rate of 500 r min⁻¹ during the reaction. CO₂ (3 vol%) was supplied at a constant concentration, in combination with nitrogen, using a mass flow controller. The gas supplied was injected into each reactor at a rate of 1,000 cm³ min⁻¹. The concentration of CO₂ was inspected at five-minute intervals using GC (gas chromatography; Agilent Technologies, model 7890A).

B. Differential reaction calorimeter (DRC)

Fig. 2 shows the configuration for the differential reaction calorimeter (DRC) experiment. The reactor had a double jacket structure with an inner volume of 250 mL. A total of 150 mL of the absorbent was injected into each reactor. The temperature in the reactors was kept constant during the reaction time using a thermostat. Two types of reactors were used: a reference reactor and a measurement reactor. The gas injected into the reactor was 3 vol% CO₂ mixed gas. In order to maximize the reaction area of the absorbent, a sparger was used to give the injection a constant flow rate of 150 cm³ • min⁻¹. The absorbent was stirred at a constant rate of 250 r • min⁻¹ over the entire reaction time. Gas chromatography was used to analyze the concentration of CO₂ exhausted after reaction with the absorbent inside the reactor. The absorbent underwent an exothermic reaction as it reacted with CO₂; this reaction was measured in real time by the thermocouple located inside the reactor. Differences in the measured reaction heat were stored on the computer in real time. The details of the experimental procedure are available in a previous report [22].

IV. THEORETICAL FOUNDATIONS

A. Measurement of CO₂ capacity using CSTR

The moles of CO₂ absorbed by the absorbents ($n_{\text{absorbed CO}_2}$) at each measurement point was calculated using

Equation (1)-(3).

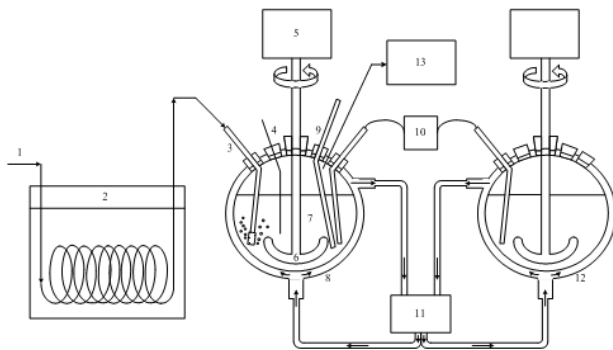


Figure 2. Schematic diagram of differential reaction calorimeter: 1) CO₂ gas (3 vol% CO₂ / balanced N₂), 2) Water bath, 3) Inlet gas port, 4) Optional probe, 5) Motor, 6) impeller, 7) Absorbent, 8) Double jacketed reactor, 9) Calibration probe, 10) Temperatures and ΔT measurements, 11) Thermostat, 12) Reference reactor, 13) Gas chromatography.

$$n_{CO_2,out} = \frac{P_{CO_2,in} \times V_{CO_2,in}}{R \times T_{CO_2,in}} \quad (1)$$

$$n_{CO_2,out} = \frac{P_{CO_2,out} \times V_{CO_2,out}}{R \times T_{CO_2,out}} \quad (2)$$

$$n_{absorbed\ CO_2} = n_{CO_2,in} - n_{CO_2,out} \quad (3)$$

$$n_{absorbed\ CO_2} = \int_0^t n_{absorbed\ CO_2} dt \quad (4)$$

where PCO₂ (atm), VCO₂ (mol/min), and TCO₂ (K) are the partial pressure, volume, and temperature of CO₂, respectively. The subscripts, 'in' and 'out' indicate inlet and outlet. CO₂ absorption capacity at saturated point was calculated using equation (4).

B. Measurement of the heat of reaction using DRC

The measurement of the heat of reaction between the absorbent and CO₂ was conducted three times: (1) calibration time before the CO₂ reaction, (2) for the CO₂ reaction, and (3) calibration time after the CO₂ reaction. The heat of reaction is indicated by temperature changes per unit time in the reference reactor and the measurement reactor. As can be seen in equation (5), the heat of reaction calibration factor Q (kJ) can be calculated using the reaction-heat-transfer coefficient (UA; W • K⁻¹) and the cumulative time changes (ΔT; K).

$$Q_{cal(1)} = UA_1 \times \int_{t_0}^{t_{end}} \Delta T dt \quad (5)$$

The UA was calculated by injecting constant energy via the calibration probe; in this study, the measurement was made three times. The heat of reaction calibration after the reaction was calculated in the same way as the heat of reaction calibration before reaction. As shown in equation (6), the total heat of reaction calibration within the reactor

was calculated as the arithmetic mean of the heat of reaction calibration before the reaction and the heat of reaction calibration after the reaction.

$$UA_{average} = \frac{UV_1 + UV_2}{2}$$

In order to measure the heat of reaction between CO₂ and absorbent, the enthalpy of the standard state was measured based on the heat of reaction per mole of CO₂, and was found to be 40 °C.

V. RESULTS AND DISCUSSION

A. CO₂ absorption capacity

The CO₂ absorption capacity was expressed in mol of CO₂ dissolved in the absorbent per mol of absorbent (mol CO₂ • mol absorbents⁻¹). Absorbents with high absorption capacity can dissolve large amounts of CO₂ in the CO₂ capture process and can thereby reduce operating cost.

The CO₂ absorption capacity was measured to evaluate the absorption performance of each absorbent. The breakthrough curve of CO₂ is shown in Fig. 3–5 at the reaction temperature of 40–80 °C. In this figure, the y-axis is the ratio of the concentration of injected CO₂ (C_i) to the concentration of

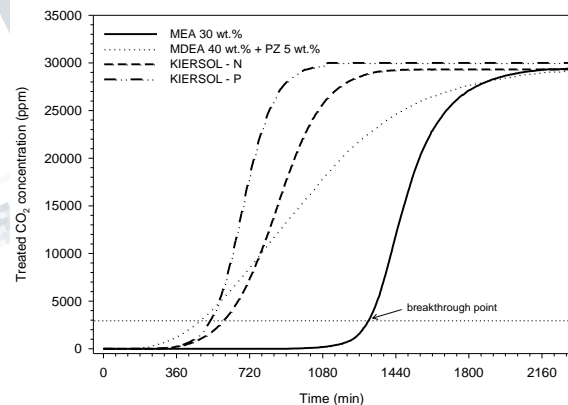


Figure 3. CO₂ absorption curve of absorbents at 40 °C.

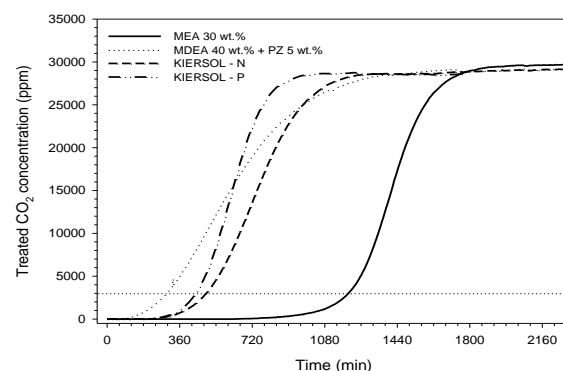


Figure 4. CO₂ absorption curve of absorbents at 60 °C.

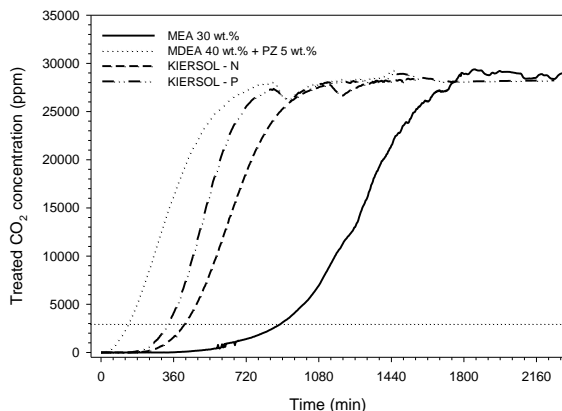


Figure 5. CO₂ absorption curve of absorbents at 80 °C emitted CO₂ (C_o), and the x-axis is the reaction time of the CO₂ and absorbent. In general, the point at which the outlet concentration is 10% of the inlet concentration is called the breakthrough point. As shown in Fig. 3–5, the breakthrough point is reached in a short time as the temperature increases. From these results, it can be shown that the amount of absorption of CO₂ depends on the reaction temperature. Table 1 shows the amount of absorbed CO₂ in each absorbent at different temperatures. The maximum CO₂ capacity of a primary amine such as MEA is generally limited to 0.5 mol CO₂ · mol amine⁻¹ due to formation of MEA carbamate (MEACOO⁻) and protonated MEA (MEA⁺H⁺). However, the absorption capacity of the MEA in this experiment was 0.74 mol CO₂ · mol amine⁻¹, which is higher than the theoretical value.

Table 1. CO₂ absorption capacity of each absorbent at temperatures from 40 to 80 °C

Absorbents	CO ₂ absorption capacity (mol CO ₂ · mol absorbent ⁻¹)		
	40 °C	60 °C	80 °C
MEA	0.74	0.70	0.64
α-MDEA	0.63	0.38	0.23
KIERSOL-P	1.14	0.98	0.81
KIERSOL-N	1.17	1.00	0.84

These results were affected by the simulated pressure of the absorber (9.50–9.52 bar). The results for KIERSOL-P and KIERSOL-N at 40 °C were 1.14 and 1.17 mol CO₂ · mol absorbent⁻¹, respectively. KIERSOL-P showed 1.54 times greater CO₂ absorption than MEA and 1.81 times greater CO₂ absorption than α-MDEA. The difference in CO₂ absorption capacity at 60 °C was greater than at 40 °C. And, the difference in CO₂ absorption capacity at 60 °C was higher than at 40 °C. KIERSOL-P showed 1.40 times greater CO₂ absorption capacity than MEA, and 2.58 times greater CO₂ absorption capacity than α-MDEA. The

CO₂ concentration remains low (< 20 ppm) after the absorbent. The curve of CO₂ in a low range of concentration is shown in Fig. 6-8, and the time is shown in Table 2 until the concentration of CO₂ reaches 20 ppm.

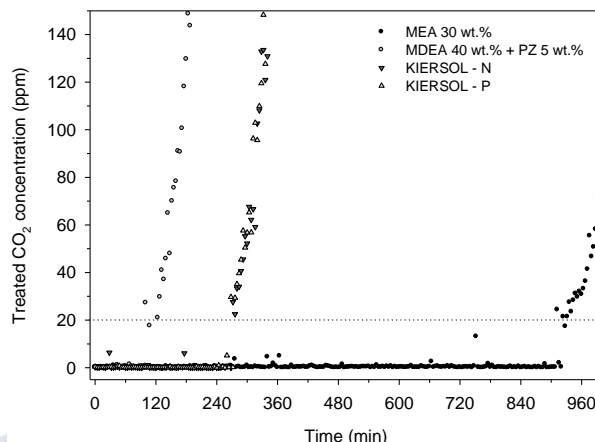


Figure 6. Initial CO₂ concentration for CO₂ absorption curve at 40 °C.

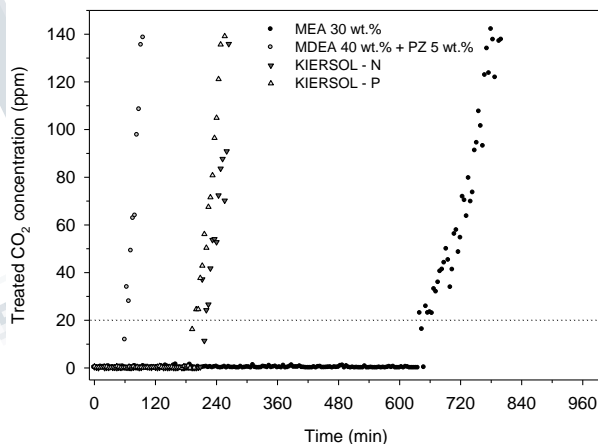


Figure 7. Initial CO₂ concentration for CO₂ absorption curve at 60 °C.

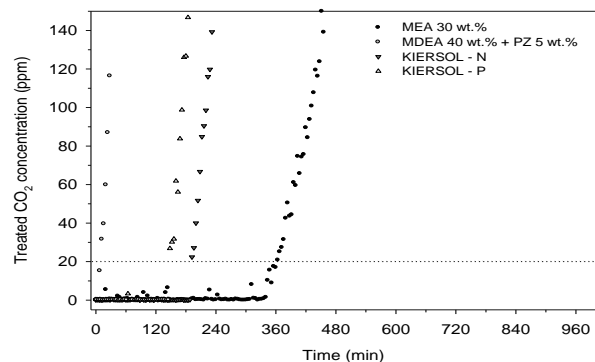


Figure 8. Initial CO₂ concentration for CO₂ absorption curve at 80 °C.

Table 2. Interval for absorbent to reach CO₂ concentration of 20 ppm.

Temperature (°C)	Interval (min)			
	MEA	MDEA+PZ	KIERSOL-N	KIERSOL-P
40	912	100	272	268
60	640	64	212	200
80	364	12	192	148

MEA provided the highest absorbent concentration at which the concentration of CO₂ was kept below 20 ppm.

Interval of absorbents with a CO₂ concentration of less than 20 ppm increased following the order MEA >

MDEA > KIERSOL-N > KIERSOL-P.

A. Heat of reaction

High CO₂ absorption rate, high cyclic capacity and low reaction heat are required to reduce the energy requirement in the CO₂ capture process [23]. In general, the heat of reaction accounts for more than 50% of the total energy requirement and is an important indicator for evaluating the performance of the absorbent. As the reaction between CO₂ and absorbents is reversible reaction, it is possible to anticipate the heat of adsorption by measuring the heat of endothermic reaction produced during the reaction between CO₂ and absorbents. The heat of reaction is the energy (kJ • mol⁻¹) that has increased through exothermic reaction per mol of CO₂ of each absorbent. Kim et al. found that when 30wt% MEA and CO₂ were made to react with each other at 40°C, the heat of reaction was 87.098 kJ • mol⁻¹ [24], and Carson et al. reported that the reaction between 30 wt% MEA and CO₂ at 25 °C resulted in the heat of reaction 83.15kJ • mol⁻¹ [24]. The results of this study showed that the heat of reaction of MEA was 96.00 kJ • mol⁻¹, which was higher than previous report. Although preceding research was conducted using 10-30 vol% CO₂ based on flue gases of the power plant, this study used low concentration CO₂ (3 vol%) of petrochemical process. The heat of reaction of MEA was 96.00 kJ • mol⁻¹ and that of α-MDEA was 68.22 kJ • mol⁻¹. As a result of the experiment, while the heat of reaction of KIERSOL-N and P were similar to that of α-MDEA, it was 0.73-0.65 times lower than that of MEA. As a result of measuring the heat of reaction, it could be found that KIERSOL-N and P were better than MEA in the aspects of absorption capacity and heat of reaction.

Table 3. Heat of absorption of saturated CO₂ at 40 °C

Absorbent	Absorbed CO ₂ (mol)	CO ₂ loading (CO ₂ mol • absorbent mol ⁻¹)	Enthalpy (ΔH: kJ • mol ⁻¹)
MEA	0.356	0.48	96.00
α-MDEA	0.145	0.25	68.22
KIERSOL-P	0.137	0.65	69.76
KIERSOL-N	0.160	0.59	62.83

VI. CONCLUSIONS

We assessed CO₂ absorption capacity, low concentration duration of CO₂, and the heat of reaction between absorbents and CO₂ in order to control 3vol.% CO₂ emitted during the acetic acid production process under ultra-low concentration 20ppm. As a result of the experiment, the absorption capacity of KIERSOL-N and KIERSOL-P at 40°C was 1.14-1.17 mol CO₂ • mol absorbent⁻¹, which was rather higher than that of MEA (0.74 mol CO₂ • mol absorbent⁻¹) or MDEA (0.63 mol CO₂ • mol absorbent⁻¹). Although MEA kept the concentration of CO₂ under 20ppm longer than the others, KIERSOL-N and KIERSOL-P emitted low concentration CO₂ longer than MDEA. As for the heat of reaction, α-MDEA, KIERSOL-N and KIERSOL-P showed similar results, and MEA was found to have very high heat of reaction. The study results indicate that KIERSOL-N and KIERSOL-P have high absorption capacity, low heat of reaction, and long low concentration carbon dioxide duration. Thus, KIERSOL-N and KIERSOL-P are expected to improve the efficiency of the acetic acid production process.

V. ACKNOWLEDGEMENTS

This work was supported by the Energy Demand Management Technology Program of the Korea Institute of Energy Technology Evaluation and Planning (KETEP), granted financial resource from the Ministry of Trade, Industry and Energy, Republic of Korea. (No. 20172010202060)

REFERENCES

- [1] M. T. Ashtiany, A. M. Rezaee, and M. R. Jafari Nasr, "An investigation on the effects of iodide salts in iridium catalyst in methanol carbonylation process" Journal of Applied Chemical Researches, vol. 4, pp. 11-18, August 2010.
- [2] HIS Market "Monochloroacetic acid" Chemical economics handbook, November 2016.
- [3] Grand view research, "Acetic Acid Market Analysis By Application (VAM, Acetic Anhydride, Acetate Esters, PTA) And Segment Forecasts To 2022", ISBN: 978-1-68038-0774-4, July 2015.
- [4] S. Bhaduri, and D. Mukesh "Homogeneous Catalysis: Mechanisms and Industrial Applications" John Wiley & Sons, 2014.
- [5] A. Haynes, P. M. Maitlis, G. E. Morris, G. J. Sunley, H. Adams, P. W. Badger, C. M. Bowers, D. B. Cook, P. I. P.

- Elliott, T. Ghaffar, H. Green, T. R. Griffin, M. Payne, J. M. Pearson, M. J. Taylor, P. V. Vickers, and R. J. Watt, "Promotion of Iridium-Catalyzed Methanol Carbonylation: Mechanistic Studies of the Cativa Process" *Journal of the American Chemical Society*, vol. 126, pp. 2847-2861, February 2004.
- [6] J. H. Jones "The Cativa™ Process for the Manufacture of Acetic Acid" *Platinum Metals Rev*, vol. 44, pp. 94-105, 2000.
- [7] G. J. Sunley, and D. J. Watson, "High productivity methanol carbonylation catalysis using iridium The Cativa™ process for the manufacture of acetic acid" *Catalysis Today*, vol. 58, pp. 293-307, 2000.
- [8] P. I. P. Elliott, S. Haak, A. J. H. M. Meijer, G. J. Sunley, and A. Haynes, "Reactivity of Ir(III) carbonyl complexes with water: alternative by-product formation pathways in catalytic methanol carbonylation" *Dalton Transactions*, vol. 42, pp. 16538-16546, September 2013.
- [9] G. Borah, and D. Boruah, "Ruthenium(II), rhodium(I) and iridium(I) complexes with [p-(N,N-dimethylamino)phenyl]diphenylphosphine ligand: Synthesis, characterization and rhodium-catalysed carbonylation of methanol" *Indian Journal of Chemistry*, vol. 52A, pp. 334-341, March 2013.
- [10] S. A. Al-Sayari, "Recent Developments in the Partial Oxidation of Methane to Syngas" *The Open Catalysis Journal*, vol. 6, pp. 17-28, June 2013.
- [11] A. L. Kohl, and R. B. Nielsen, "Gas Purification" Gulf Publishing Company, ISBN: 978-0-88415-220-0, 1997.
- [12] J. H. Choi, Y. E. Kim, S. C. Nam, S. H. Yun, Y. I. Yoon, and J-H Lee, "CO₂ absorption characteristics of a piperazine derivative with primary, secondary, and tertiary amino groups" *Korean J. Chem. Eng.* Vol. 33, pp. 3222-3230, June 2016.
- [13] C. Han, K. Graves, J. Neathery, and K. Liu, "Simulation of the Energy Consumption of CO₂ Capture by Aqueous Monoethanolamine in Pilot Plant" *Energy Environment Research*, vol. 1, pp. 67-80, December 2011.
- [14] Y. E. Kim, J. H. Choi, S. C. Nam, and Y. I. Yoon, "CO₂ Absorption Characteristics in Aqueous K₂CO₃ / Piperazine Solution by NMR Spectroscopy" *Industrial & Engineering Chemistry Research*, vol. 50, pp. 9306-3913, June 2011.
- [15] J. Davison, "Performance and costs of power plants with capture and storage of CO₂" *Energy*, vol. 32, pp. 1163-1176, July 2007.
- [16] S. H. Yun, Y. E. Kim, J. H. Choi, S. C. Nam, J. Chang, and Y. I. Yoon, "CO₂ absorption, density, viscosity and vapor pressure of aqueous potassium carbonate + 2-methylpiperazine" *Korean Journal of Chemical Engineering*, vol. 33, pp. 3473-3486, December 2016.
- [17] S. Y. Khan, M. Yusuf, and A. Malani, "Selection of Amine in Natural Gas Sweetening Process for Acid Gases Removal: A Review of Recent Studies" *Petroleum & Petrochemical Engineering Journal*, vol. 1, pp. 1-7, June 2017.
- [18] H. Kierzkowska-pawlak, and A. Chacuk, "Kinetics of Carbon Dioxide Absorption into Aqueous MDEA Solutions" *Ecological Chemistry and Engineering S*, vol. 17, pp. 463-475, 2010.
- [19] B. Sherman, X. Chen, T. Nguyen, Q. Xu, H. Rafique, S. A. Freeman, A. K. Voice, and G. T. Rochelle, "Carbon Capture with 4 m Piperazine / 4 m 2-methylpiperazine" *Energy Procedia*, vol. 37, pp. 436-447, 2013.
- [20] Y. E. Kim, J. H. Choi, S. C. Nam, and Y. I. Yoon, "CO₂ absorption capacity using aqueous potassium carbonate with 2-methylpiperazine and piperazine" *Journal of Industrial and Engineering Chemistry*, vol. 18, pp. 105-110, January 2012.
- [21] Y. I. Yoon, Y. E. Kim, S. C. Nam, S. K. Jeong, S. Y. Park, M. H. Youn, and K. T. Park. "Characteristics of CO₂ capture system using KIERSOL in the LNG flue gas" *Energy Procedia*, vol. 63, pp. 1745-1750, 2014.
- [22] J. H. Choi, S. H. Yoon, Y. E. Kim, Y. I. Yoon, and S. C. Nam, "The Effect of Functional Group Position of the Piperidine Derivatives on the CO₂ Absorption Characteristics in the (H₂O-Piperidine-CO₂) System" *Korean Chemical Engineering Research*, vol. 53, pp. 57-63, November 2014.
- [23] F. A. Chowdhury, H. Yamada, T. Higashii, K. Goto, and M. Onoda, "CO₂ Capture by Tertiary Amine Absorbents: A Performance Comparison Study", *Industrial & Engineering Chemistry Research*, vol. 52, pp. 8323-8331. 2013.
- [24] I. Kim, and H. F. Svendsen, "Heat of Absorption of Carbon Dioxide (CO₂) in Monoethanolamine (MEA) and 2-(Aminoethyl) Ethanolamine (AEEA) Solutions." *Industrial & Engineering Chemistry Research*. vol. 46, pp. 5803-5809, July 2007.

[25] J. K. Carson, K. N. Marsh, and A. E. Mather, "Enthalpy of Solution of Carbon Dioxide in (Water + Monoethanolamine, or Diethanolamine, or N-Methyldiethanolamine) and (Water + Monoethanolamine + N-Methyldiethanolamine) at T= 298.15 K." The Journal of Chemical Thermodynamics, vol. 32, pp. 1285-1295. September 2000.

I.

